

Penetration of Titanium Tetraisopropoxide into Mesoporous Silica Using Supercritical Carbon Dioxide

Narihito Tatsuda,^{*,†,‡} Yoshiaki Fukushima,^{†,‡} and Hiroaki Wakayama[‡]

Toyota Technological Institute, 2-12-1 Hisakata, Tenpaku, Nagoya, 458-8511 Japan, and Toyota Central Research and Development Labs, Inc., Nagakute, Aichi, 480-1192 Japan

Received May 28, 2003. Revised Manuscript Received February 10, 2004

A penetration of titanium tetraisopropoxide (TTIP) and a reaction with silanol groups to form TiO₂ layers on the inner surface of mesoporous silica samples were studied. Influence of the solvent on the penetration behavior was discussed. The TTIP could penetrate into the mesopores with diameters of 2.3 and 2.7 nm and the pore size was decreased by the TTIP coating, only when supercritical CO₂ were used as solvent. The pore size change was also observed for mesopores larger than 3.5 nm by using both supercritical CO₂ and liquid 2-propanol. These behaviors are reasonably discussed not only by the relation between the pore diameter and the solvated TTIP molecular size, but also by the adsorption energy of the solvent molecules on the silica surface. A difference of the penetration behavior of TTIP from that of tetraethoxyorthosilane (TEOS) suggested that the reactivity with silanol groups on the silica surface also affected the penetration behavior.

Introduction

Preparation of thin film and porous materials with monolayer or nanometer-scale thicknesses is attracting much attention due to their wide applications in catalyses, etc. Methods to prepare ultrathin layers of metal oxide gels were developed by Ichinose et al.¹ and Fleinfeld et al.² Several reports have described the modification to mesoporous silica by coating^{3–5} metal oxides onto the pore surface using organometallic precursors or by incorporating^{6–10} metal oxides into the silica frameworks.

Supercritical fluids may have some advantages as a solvent for coating processes because of their high diffusivity, noncondensation, and weak solvation property with solutes. This coating process^{11–15} using a supercritical fluid is applicable to metal and metal

oxides, such as platinum,¹¹ silica,^{12–13} titanium dioxide,¹⁴ and alumina¹⁴ on activated carbon. Wakayama reported that tetraethyl orthosilicate (TEOS) penetrates by supercritical CO₂ solvent into mesopores with less than 25-nm pores.¹⁵

The molecular size of the precursors, the reactivities with surface silanol groups of substrates, and the solvation properties are also principal factors for coating using supercritical fluids. As titanium oxides have a potential for many applications such as photochemical reactions or electric capacitors, penetration into thin spaces of the precursors of TiO₂ should be important for developing the TiO₂ thin film coating processes.

In this paper, the penetration of titanium tetraisopropoxide (TTIP) using supercritical CO₂ solvent was studied, and the influence of molecular size and reactivity with the pore surface silanol group on the coating process was discussed.

Experimental Section

Materials. TTIP with a purity of 99.999 wt %, purchased from Kojundo Chemical Lab Co., was used as a precursor for TiO₂ without further purifications. 2-Propanol (IPA) with a purity of 99 wt % (Wako Junyaku Co.) was dehydrated with molecular sieves 3A until its water content was less than 100 ppm, which was confirmed by Karl Fischer method. CO₂ with a purity of 99.99 wt % was used as a solvent. Mesoporous silicas, FSM-*n* (*n* = 8, 10, 12, 16, 18), were prepared with cationic surfactants containing alkyl chains in the molecules.¹⁶ The value *n* denotes the number of carbons in the alkyl chains of the surfactant. The average pore diameter *d*_{ave}, pore volume

* To whom correspondence should be addressed. E-mail: tatsuda@mosk.tytlabs.co.jp. Fax: +81-561-63-6156.

[†] Toyota Technological Institute.

[‡] Toyota Central Research and Development Labs.

(1) Ichinose, I.; Senzu, H.; Kunitake, T. *Chem. Mater.* **1997**, *9*, 1296–1298.

(2) Fleinfeld, E.; Ferquson, G. S. *Mater. Res. Soc. Symp. Proc.* **1994**, *351*, 419–424.

(3) Maschmeyer, T.; Rey, F.; Sankar, G.; Thomas, J. M. *Nature* **1995**, *378*, 159–162.

(4) Aronson, B. J.; Blanford, C. F.; Stein, A. *Chem. Mater.* **1997**, *9*, 2842–2851.

(5) Luan, L.; Maes, E. M.; Heide, P. A. W.; Zhao, D.; Czernuszewicz, R. C.; Kevan, L. *Chem. Mater.* **1999**, *11*, 3680–3686.

(6) Tanev, P.; Chibwe, M.; Pinnavaika, T. J. *Nature* **1994**, *368*, 321–323.

(7) Zhang, W.; Pinnavaia, T. J. *Catal. Lett.* **1996**, *38*, 261–265.

(8) Alba, M. D.; Luan, Z.; Klinnowski, J. J. *Phys. Chem.* **1996**, *100*, 2178–2182.

(9) Morey, M.; Daviason, A.; Stucky, G. *Microporous Mater.* **1996**, *6*, 99–104.

(10) Tatsumi, T.; Koyano, K. A.; Igarashi, N. *Chem. Commun.* **1998**, 325–326.

(11) Wakayama, H.; Fukushima, Y. *Chem. Commun.* **1999**, 391–392.

(12) Wakayama, H.; Fukushima, Y. *Chem. Mater.* **1999**, *12*, 756–761.

(13) Fukushima, Y.; Wakayama, H. *J. Phys. Chem. B* **1999**, *103*, 3062–3064.

(14) Wakayama, H.; Itahara, H.; Tatsuda, N.; Inagaki, S.; Fukushima, Y. *Chem. Mater.* **2001**, *13*, 2392–2396.

(15) Wakayama, H.; Fukushima, Y. *Proceedings of the 5th International Conference on Solvo-Thermal Reactions East Brunswick*; 2002; pp 189–194, conference committee.

(16) Inagaki, S.; Koiwai, A.; Suzuki, N.; Fukushima, Y.; Kuroda, K. *Bull. Chem. Soc. Jpn.* **1996**, *69*, 1229.

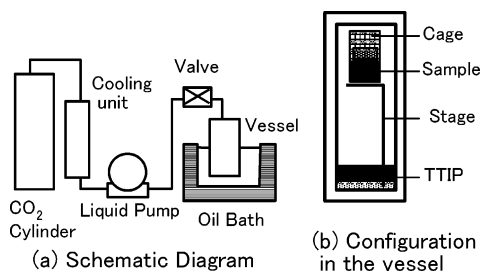


Figure 1. Apparatus for the experiment with supercritical carbon dioxide.

Table 1. Properties of the Mesoporous Silicas FSM Calculated from Desorption Branches of Nitrogen Adsorption Isotherms Using α_s Plot Analysis

material	d_{ave} (nm)	V_p (ml/g)	S_{total} (m ² /g)	S_{ex} (m ² /g)
FSM-8	1.6	0.35	892	12
FSM-10	2.3	0.43	778	32
FSM-12	2.7	0.59	923	42
FSM-16	3.5	0.72	909	85
FSM-18	3.7	0.85	959	52

V_p , total specific surface area S_{total} , and external specific surface area S_{ex} are listed in Table 1. V_p , S_{total} , and S_{ex} are estimated by α_s plot analysis using an adsorption isotherm of N₂ at 77 K. The d_{ave} was calculated by

$$d_{ave} = 4V_p / (S_{total} - S_{ex}) = 4V_p / S_{in} \quad (1)$$

where S_{in} is the internal specific surface area.

Coating of TiO₂ on Mesoporous Silica. A glovebox filled with nitrogen and controlled to a dew point of less than 183 K, in which the moisture level was less than 0.6 ppm, was used for preparing samples. The powdered FSMs were placed in the glovebox for 1 h to decrease the water concentration on the FSMs to less than 0.1 wt %. A vessel with 70-mL capacity, shown in Figure 1b, was used for the supercritical fluid (SCF) treatment. The FSM-*n* (0.5 g) held in the stainless cage was set at the upper part of the vessel to keep away from the liquid TTIP 1.42 g (0.0050 mol) at the bottom. CO₂ from the cylinder was condensed by cooling and induced by a liquid pump into the vessel up to 2 MPa, using the apparatus shown in Figure 1a. Then, a valve was gradually opened to reduce the pressure inside the vessel to 0.2 MPa. This process was repeated 3 × to replace N₂ in the vessel by CO₂. Furthermore, the vessel was immersed in an oil bath held at 393 K, and CO₂ was further added to control the pressure up to 20 MPa for 3 h, followed by rapid cooling to 298 K. After releasing the vessel pressure to atmospheric pressure, the samples were taken out and dried at 378 K for 12 h in a hot dry oven. Treatments with liquid IPA were also performed in the above-mentioned glovebox. FSM-*n* (0.5 g) was put into an IPA (30 g) solution of TTIP (0.0050 mol) in a glass beaker (100 mL) and stirred with a magnetic stirrer at 298 K for 18 h. The treated samples were filtered from the solution and rinsed with the liquid IPA 2 ×. These samples were also dried at 378 K for 12 h in a hot dry oven.

Analyses. The atomic ratio Ti/Si was estimated using an X-ray fluorescence spectrometer (XRF-1500PC, SHIMADU Co.). The data were calibrated with the reference sample using 80 wt % SiO₂ and 20 wt % TiO₂. The nitrogen adsorption and desorption isotherms at 77 K were measured by an Autosorp-1-MP (Quantacrome Instruments Co.) after degassing the samples at 423 K in 10⁻⁶ Torr for 3 h. An α_s plot analysis and Barrett, Joyner, and Halenda (BJH) method were used to estimate the pore size. Because the result of the pore size estimated by the α_s method well-represented the previous results¹⁷ using the XRD method, the α_s plot was used in this

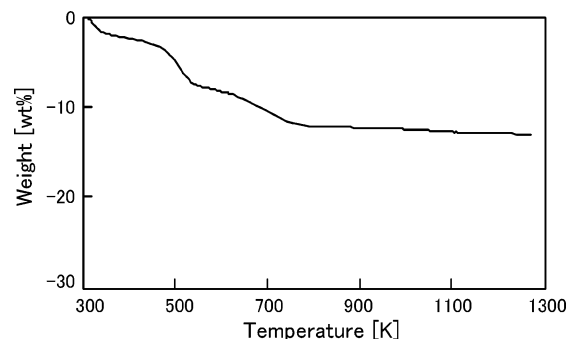


Figure 2. Thermogravimetric curve for SCF-treated FSM-16.

work, and the BJH method was employed only for estimating the relative change of pore size due to the treatments.

Infrared (IR) spectra were collected by a Fourier transform infrared spectrometer (Avatar 380 FT-IR, Thermo Nicolet Co.) using the attenuated total reflection (ATR) method with a diamond crystal in order to estimate an amount of the methyl group from TTIP in the treated samples. The powdered samples were coated on the above-mentioned diamond crystals for the IR measurements in the air. The silanol at the surface of the mesoporous silicas was expected to react with the solvent or TTIP during the TTIP coating treatment. Mesoporous silica samples were also treated with the liquid IPA at 523 K in a sealed vessel for 3 h for comparison.

An amount of the organic part in the treated samples was estimated by thermogravimetric (TG) analyses in the air flow. The typical TG result is shown in Figure 2. As the weight loss below the temperature at 448 K would be attributed to dehydration, an organic part was calculated by

$$A_{org} = (W_{448K} - W_{873K}) / W_{448K} \quad (2)$$

where W_{448K} and W_{873K} are weights of the samples at 448 and 873 K in air, respectively.

The structure of the TiO₂-treated mesoporous silicas FSM-16 with 3.5 nm pore diameter was studied by X-ray powder diffraction using a Rigaku RINT 1500V with Cu K α of 40 kV and 350 mA at a step scan (6 s/0.04 $^\circ$ (2 θ)) with divergency slit (DS) of 0.5 $^\circ$, scattering slit (SS) of 0.5 $^\circ$, and receiving slit (RS) of 0.15 mm, and solid state ²⁹Si-MAS NMR with a Bruker AVANCE-400 spectrometer at 79.494 MHz and spinning of 5 kHz using pulses at 90-s intervals.

Adsorption of CO₂ at High Pressure. The CO₂ adsorption-desorption isotherms were gravimetrically collected with a FSM-AD-H100 instrument designed for adsorption isotherms at high pressures, containing a vessel for high pressure, a microbalance out of the vessel, and the magnetic couplings for transmitting the weight change of samples in the vessel to the balance. A titanium sinker whose exact volume and weight were known was also set up in the high-pressure vessel for calibrating the buoyancy by adsorbate gases under high pressure. As the buoyancy effect could not be neglected under a high-pressure environment, an apparent weight change, W_{sam} , should be corrected to obtain an excess adsorbed amount, m_{ex} , in pores by eq 3:

$$m_{ex} = W_{sam} + \rho_{bulk} V_{sol} \quad (3)$$

where ρ_{bulk} is the bulk density of CO₂ under the experimental pressure and V_{sol} is the volume of the sample, which is determined by the helium adsorption measurement. The bulk density of CO₂, ρ_{bulk} , is estimated by the apparent weight change of the sinker and the sinker volume. As adsorption occurs on both the inside and outside of the pore, a total amount of the adsorbate in pores, m_p , can be calculated by the following equation:

$$m_p = \alpha m_{ex} + \rho_{bulk} V_p \quad (4)$$

(17) Inagaki, S.; Sakamoto, Y.; Fukushima, Y.; Terasaki, Y. *Chem. Mater.* **1996**, *8*, 2089.

Table 2. Parameters for Benedict–Webb–Rubin Equation for Carbon Dioxide¹⁸

parameter	units	value
A_0	$[(\text{dm}^3\text{mol}^{-1})^2 \text{MPa}]$	0.277369
B_0	$[(\text{dm}^3\text{mol}^{-1})]$	4.9901×10^{-2}
C_0	$[(\text{dm}^3\text{mol}^{-1})^2 \text{K}^2 \text{MPa}]$	1.40403×10^4
a	$[(\text{dm}^3\text{mol}^{-1})^3 \text{MPa}]$	1.38627×10^{-2}
b	$[(\text{dm}^3\text{mol}^{-1})^2]$	4.1239×10^{-3}
c	$[(\text{dm}^3\text{mol}^{-1})^3]$	1.49180×10^4
α'	$[(\text{dm}^3\text{mol}^{-1})^3]$	8.47×10^{-5}
γ	$[(\text{dm}^3\text{mol}^{-1})^3]$	5.394×10^{-3}

where V_p is the pore volume and α is the ratio of the excess adsorbed amount inside the pore to the total excess adsorbed amount, which is approximated to the ratio of the internal specific surface area and the total specific surface area.

$$\alpha = S_{\text{in}}/S_{\text{total}} \quad (5)$$

The average density of the adsorbate in the pore is estimated by

$$\rho_p = m_p/V_p \quad (6)$$

Evaluation of Characteristic Curves. The characteristic curve for the adsorption of CO₂, which is the relation between the adsorption potential and the volume of adsorbed layer, V_{ad} , were evaluated from the adsorption isotherms from 267 to 320 K. When the pressure of the adsorbed layer was assumed to be equal to the saturated vapor pressure, P_0 , an amount of Gibbs free energy change due to the adsorption, i.e., adsorption potential, ϵ , is given by

$$\epsilon = RT \log(P_0/P) \quad (7)$$

where R is the gas constant, T is the temperature, and P is the pressure in the bulk fluid. Because the saturated vapor pressure could not be defined above the critical temperature, P_0 in eq 7 should be replaced by the quasi-saturated vapor pressure P_s . The P_s was calculated by the Antonius equation.

$$\log P_s = 7.7693 - \frac{1647.77}{T + 251.53} \quad (8)$$

The pressure should be replaced by fugacity, f , because CO₂ at such a high pressure has nonideal gas properties. The fugacity is estimated using the Benedict–Webb–Rubin (BWR) equation¹⁸

$$P = \frac{RT}{V} + \frac{B_0RT - A_0 - C_0/T^2}{V^2} + \frac{bRT - a}{V^3} + \frac{a\alpha'}{V^6} + \frac{c}{T^2V^3} \left(1 + \frac{\gamma}{V^2}\right) \exp\left(-\frac{\gamma}{V^2}\right) \quad (9)$$

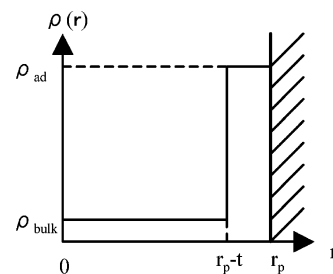
where A_0 , B_0 , C_0 , a , b , c , α' , and γ are the virial parameters as shown in Table 2. The fugacity is estimated by the following equations.

$$\log \gamma' = \int_0^P (RT/P - V) dP \quad (10)$$

$$f = \gamma' P \quad (11)$$

The eq 7 was replaced by the following equation using a f_s corresponding to the quasi-saturated vapor pressure.

$$\epsilon = RT \log(f_s/f) \quad (12)$$

**Figure 3.** Slab approximation model in a mesopore.**Table 3. Atomic Ratios of Ti/Si Evaluated by X-ray Fluorescence Analysis**

material	SCF-CO ₂ treated		liquid IPA treated	
	as treated	calcined	as treated	calcined
FSM-8	0.070	0.089	0.009	0.009
FSM-10	0.118	0.119	0.019	0.024
FSM-12	0.131	0.131	0.040	0.039
FSM-16	0.141	0.134	0.150	0.142
FSM-18	0.123	0.118	0.130	0.138

A density profile is simplified as shown in Figure 3, where the densities of a nonadsorbed vapor phase and an adsorbed layer are approximated to that of the bulk phase and a density of the liquid phase, respectively. According to these approximations, V_{ad} is estimated by

$$V_{\text{ad}} = \alpha m_{\text{ex}} / (\rho_{\text{ad}} - \rho_{\text{bulk}}) \quad (13)$$

where m_{ex} is the adsorption excess, ρ_{ad} is the density of the adsorbed phase, and ρ_{bulk} is density of the bulk phase. The m_{ex} and ρ_{bulk} can be obtained experimentally. At the temperature where T is lower than the critical temperature, T_c , ρ_{ad} is determined as the density at which the slope of the adsorption isotherm decreases discontinuously. At $T > T_c$, ρ_{ad} is extrapolated with the exponential function from the values of ρ_{ad} below T_c .

Result and Discussion

Titanium Amount in TTIP-Treated Porous Materials. The atomic ratios, Ti/Si, in the treated samples estimated by X-ray fluorescence analysis are shown in Table 3. For the mesoporous silicas FSM-16 ($d_{\text{ave}} = 3.5$ nm) and FSM-18 ($d_{\text{ave}} = 3.7$ nm), the apparent difference in the ratio between the SCF-treated and the liquid-IPA-treated samples was not observed. On the other hand, for the mesoporous silicas with $d_{\text{ave}} \leq 2.7$ nm, the samples treated by the SCF process had a much larger Ti compared to the samples treated by the liquid IPA solvent process.

The quantity of Ti did not decrease much by a heat treatment at 793K for 3 h. Because the boiling point of TTIP is near 493 K, these results suggested that the TTIP condensed or reacted with the silanol group on the mesoporous silicas during the coating processes.

Coverage of TiO₂ on the SiO₂ Substrate Surface. The thickness of a pore wall, t_w , is estimated with the honeycomb structure model. The distance between the centers of the neighbor pores, d_s , is the sum of the average pore diameter, d_{ave} , and the thickness of the pore wall, t_w .

$$d_s = d_{\text{ave}} + t_w \quad (14)$$

(18) Chemical Society of Japan, *Kagakubinran Kiso-hen No. 4 II-115*; Maruzen: Tokyo, Japan, 1993.

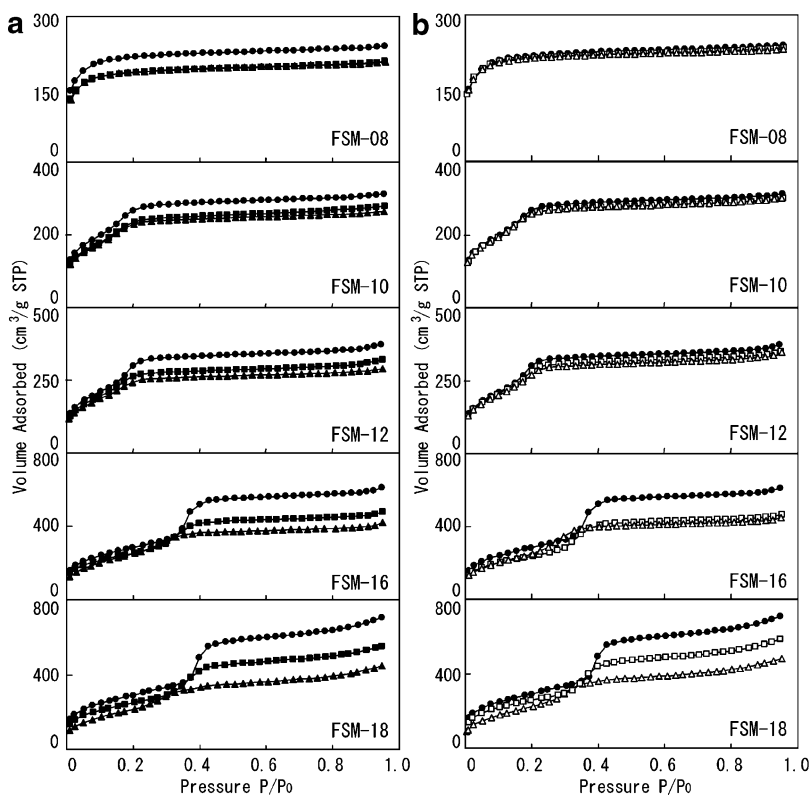


Figure 4. Adsorption isotherms of N₂ at 77 K on the FSMs: (a) samples treated with supercritical CO₂ solvent; (b) samples treated with IPA liquid solvent; ●, untreated samples; ▲, samples treated with the SCF-CO₂ solvent; ■, samples calcined after the SCF-CO₂ treatment; △, samples treated with the liquid IPA solvent; □, samples calcined after the liquid IPA treatment.

The ratio of the wall volume to the total volume, β , is obtained by eq 15.

$$\beta = \frac{V_{\text{wall}}}{V_{\text{p}} + V_{\text{wall}}} = \frac{3t_{\text{w}} \left(\frac{d_{\text{s}}}{2\sqrt{3}} - \frac{t_{\text{w}}}{2\sqrt{3}} \right) + \frac{t_{\text{w}}}{2} \frac{\sqrt{3}t_{\text{w}}}{2}}{\frac{d_{\text{s}}}{2} \frac{\sqrt{3}d_{\text{s}}}{2}} = \frac{2t_{\text{w}}d_{\text{s}} - t_{\text{w}}^2}{d_{\text{s}}^2} \quad (15)$$

and

$$t_{\text{w}} = d_{\text{s}}(1 \pm \sqrt{1 - \beta}) \quad (16)$$

Using a density of the pore wall, 2.3 g/cm³, which was obtained experimentally, the wall thickness for FSMs is estimated to be 0.9 ± 0.1 nm. These results suggested that the pore walls of the FSMs consisted of double layers of silica sheets, and most of the silicon atoms were situated on the wall surface. When the surface layers of FSMs consist of six-membered rings of SiO₄ tetrahedron, with side length of 0.26 nm, the number of Si is estimated as 8.5 atoms per 1 nm² on an average.

As the molecular size of the grafted TTIP with three isopropoxide groups is estimated as 1 nm, the maximum of TTIP which was in contact with the wall would be estimated at 1.3 atoms per 1 nm². Therefore, the maximum of Ti/Si can be estimated at 0.15. The ratios of the titanium to the silicon in the treated FSM-16 and FSM-18 were about 0.14–0.15 and 0.12–0.13, respectively. It is consistently accepted that the inner surface of these mesoporous silicas was covered by a monolayer of TTIP.

Table 4. Pore Diameter Changes (nm) Due to the Coating and the Calcination Process Estimated with Pore Size Distribution Using BJH Method

material	initial	SCF-CO ₂		liquid IPA	
		coated	calcined	coated	calcined
FSM-8 (1.6 nm) ^a	ND ^b	ND	ND	ND	ND
FSM-10 (2.3 nm) ^a	18.8	18.2	18.2	18.8	18.8
FSM-12 (2.7 nm) ^a	20.0	18.2	18.7	20.0	20.0
FSM-16 (3.5 nm) ^a	29.5	25.2	27.3	25.0	27.3
FSM-18 (3.7 nm) ^a	31.2	25.1	29.5	26.5	29.5

^a Pore diameter estimated by α_{s} plot. ^b ND, cannot be determined.

Change of a Pore Size Distribution in the Mesoporous Silicas with the Treatment. The N₂ adsorption isotherms at 77 K are shown in Figure 4. The pore size distributions estimated using the BJH method are shown in Figure 5. The changes of the pore diameter due to the coating and calcination processes were estimated by peak positions of the pore size distribution curves as shown in Table 4. Both TTIP coating treatments, using the supercritical CO₂ and the liquid IPA as the solvent, decreased the pore size by about 0.5 nm in diameter for FSM-16 ($d_{\text{ave}} = 3.5$ nm) and FSM-18 ($d_{\text{ave}} = 3.7$ nm). The pore size of the TTIP-coated sample was recovered by about 0.3 nm after calcination at 793 K for 3 h due to the decomposition of isopropoxyl groups.

The pore sizes of FSM-10 ($d_{\text{ave}} = 2.3$ nm) and FSM-12 ($d_{\text{ave}} = 2.7$ nm) were also decreased by the TTIP treatment, only when the supercritical CO₂ was used as a solvent. The difference of the pore size by the treatment is smaller compared with that for FSM-16 or FSM-18. The pore sizes of FSM-10 and FSM-12 were not changed by the treatment with the liquid solvent. These results suggest that the TTIP molecule could not

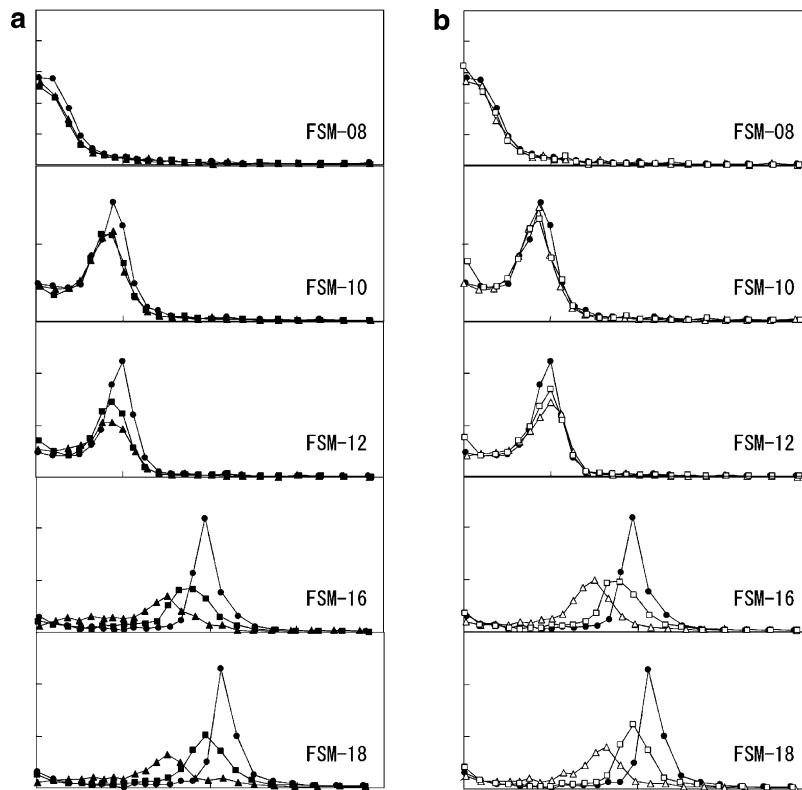


Figure 5. Pore size distributions estimated by BJH method: (a) samples treated with supercritical CO₂ solvent; (b) samples treated with IPA liquid solvent; ●, untreated samples; ▲, samples treated with SCF-CO₂ solvent; ■, the samples calcined after the SCF-CO₂ treatment; △, samples treated with the liquid IPA solvent; □, samples calcined after the liquid IPA treatment.

penetrate into the pores with diameters of 2.3 and 2.7 nm when the liquid IPA was used as a solvent. The supercritical CO₂ made the penetration possible, but the mobility of the solvated molecules is restricted in these pores, which resulted in the thinner coating layers.

For FSM-8, with an average pore diameter of 1.6 nm, the change in pore diameter was not observed even by the supercritical CO₂ treatment.

It has been reported¹⁵ that TEOS could enter in the FSM-8 by the SCF coating process. Although the larger molecular size of TTIP than TEOS would be attributed to the result, the size difference is not significant. Yoldas reported that titanium tetraalkoxide rapidly reacted with silanol groups in partially hydrolyzed silicon alkoxides with respect to the silicon alkoxides.¹⁹ A factor that is the higher reactivity of TTIP with the surface silanol should be considered. The reaction at the entrance of the pores would interrupt the further penetration of the TTIP molecules.

Influence of the Interaction of the Solvent Molecules with the Pore Surface. The molecular size of TTIP is estimated to be about 1.2 nm, which is sufficiently smaller than the pore size of the FSM-*n* samples used in this work. A solvation with the solvent molecules should be considered. However, the solvated sizes are still smaller than the pore size of FSM-10 and FSM-12. We should take into account the interaction of the solvent molecules with the surface of the silica mesopores, which was discussed by the adsorption energy of CO₂ calculated with the adsorption characteristic curves.

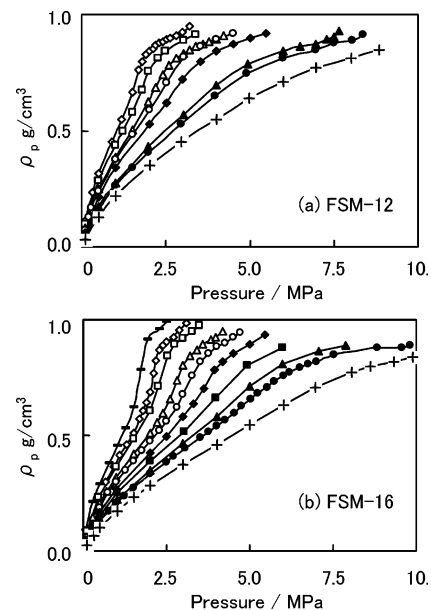


Figure 6. Adsorption isotherms for CO₂ to (a) FSM-12 and (b) FSM-16, at temperatures of - 266.7 K; ◇, 270.7 K; □, 276.2 K; △, 281.7 K; ○, 286.7 K; ◆, 292.2 K; ■, 298.4 K; ▲, 305.4 K; ●, 309.2 K; +, 319.4 K.

The adsorption isotherms for CO₂ to FSM-12 and FSM-16 at various temperatures are shown in Figure 6. The characteristic curve of the adsorption for CO₂ to FSM-12 and FSM-16 calculated from the adsorption isotherms is shown in Figure 7.

The adsorption potential for the first adsorbed layer, whose thickness is about 0.4 nm, was more than 1.2 kJ/mol. The adsorption potential for the second layer was

(19) Yoldas, B. E. *J. Non-Cryst. Solids* **1980**, *38*, 81.

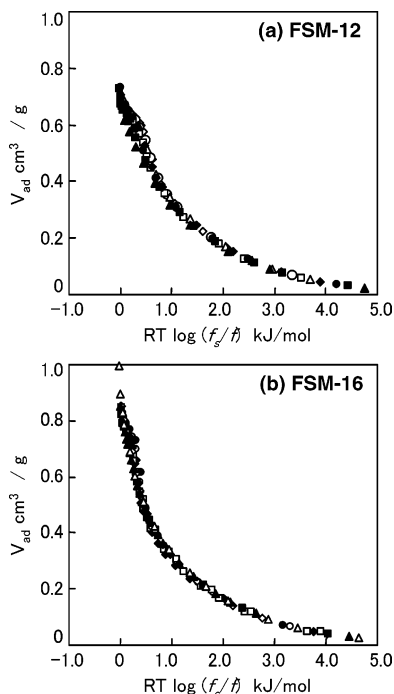


Figure 7. Characteristic curves of CO₂ adsorption on (a) FSM-12 and (b) FSM-16, at temperatures of Δ , 266.7 K; \diamond , 270.7 K; \square , 276.2 K; \triangle , 281.7 K; \circ , 286.7 K; \blacklozenge , 292.2 K; \blacksquare , 298.4 K; \blacktriangle , 305.4 K; \bullet , 309.2 K; $+$, 319.4 K.

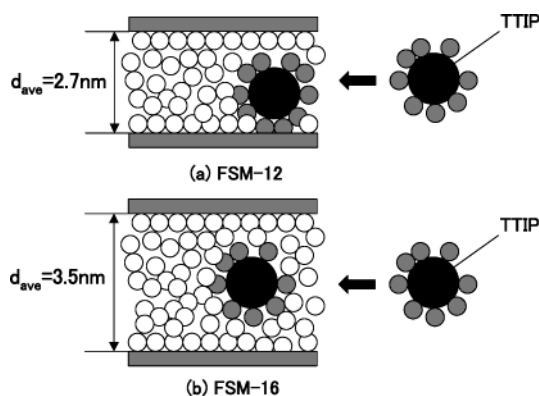


Figure 8. Tentative model for a penetration of titanium tetraisopropoxide (TTIP) solvated with CO₂ molecules, open circle; nonsolvating CO₂, shaded circle; solvating CO₂, black circle; TTIP.

0.4–1.2 kJ/mol, and that for the third layer was estimated as 0.2–0.4 kJ/mol.

The size of the TTIP molecules solvated by CO₂ would be about 2.0 nm. The solvent CO₂ molecules around the TTIP directly interacted with the surface of the mesopore of FSM-12 whose pore diameter was about 2.7 nm. The interaction between the solvent and the silica surface interrupted the diffusion of TTIP molecules into the pores, as shown in Figure 8a, and they reacted near the entrance of the pores, which prevented further penetrations.

As for FSM-16 ($d_{\text{ave}} = 3.5$ nm), the solvated CO₂ molecules were only weakly trapped as shown in Figure 8b; the solvated TTIP could penetrate into the pores even when they were solvated with CO₂ molecules.

Change of Pore Diameter by Calcination. The pore size of the mesoporous silicas was decreased by the TTIP coating treatment, and it was recovered by the

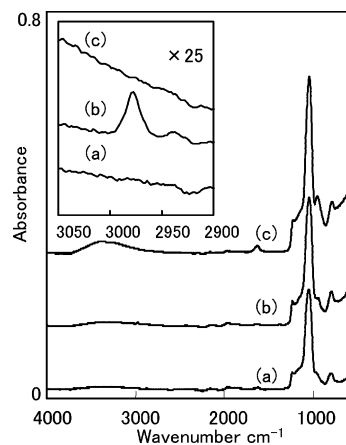


Figure 9. IR spectra of the FSM-16s: (a) untreated; (b) SCF-treated; and (c) calcined after SCF treatment.

Table 5. IR Intensity Ratios of 2980 cm⁻¹/1050 cm⁻¹ and Amount of Organic Part Estimated by TG Analysis

material	IR intensity ratio of 2980 cm ⁻¹ /1050 cm ⁻¹ × 10 ⁻²		amount of organic part (wt %)	
	as treated	calcined	as treated	calcined
FSM-8S ^a	0.678	<0.01	4.6	1.8
FSM-10S ^a	0.640	<0.01	4.6	1.3
FSM-12S ^a	0.828	<0.01	5.9	NP
FSM-16S ^a	1.460	<0.01	9.4	1.6
FSM-18S ^a	1.527	<0.01	9.7	1.3
FSM-16L ^b	0.906	<0.01	6.9	NP

^a Treated in supercritical CO₂. ^b Treated in liquid IPA. ^c NP, not performed.

following calcination at 793 K for 3 h. The IR spectra of the untreated, the SCF-treated, and the calcined FSM-16 samples are shown in Figure 9. In the spectrum of the FSM-16 after the SCF process, the two adsorption bands due to C–H stretching vibration in the methyl groups in TTIP at 2980 cm⁻¹ and the bending vibration at 1320 cm⁻¹ were observed. This result suggested that some isopropoxyl groups remain in the SCF-treated FSM-16. Ratios of the peak intensity in the IR spectra at 2980 cm⁻¹ due to the methyl group to that at 1050 cm⁻¹ by SiO₂ are listed in Table 5. The peak at 2980 cm⁻¹ disappears by the heat treatment, which means that the isopropoxyl groups were decomposed by the treatment.

The amount of the organic part estimated by the TG analysis is also shown in Table 5. There is a good linear relation between the amount of organic part and the intensity ratio of IR spectrum. This strongly suggests that the recovery of pore diameter was attributed to the decomposition of the isopropoxyl group.

Structure of TiO₂ in the Mesopores. Although few peaks from anatase or rutile crystals were observed for the sample treated with TTIP as shown in Figure 10a, those from anatase crystals were clearly observed for the calcined sample (at 793 K for 3 h in air) as shown in Figure 10b. The ²⁹Si MAS NMR spectra of the mesoporous silica in Figure 11(a) has two broad signals which were assignable to Q⁴ (from -107 to -116 ppm) and Q³ (from -98 to -101 ppm) units. Although the treatment with TTIP decreased the intensity of the Q³ peak and increased that of the Q⁴ peak, a signal at -94 to -97 ppm assigned to Si (3Si, 1Ti, that is silicon connected through oxygen bridges to three silicon atoms and one titanium atom) for microporous titanosilicate

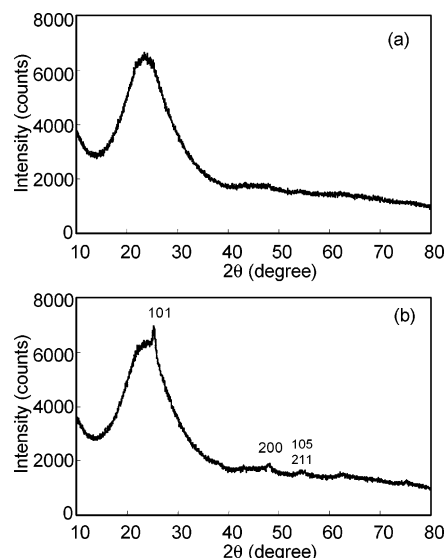


Figure 10. X-ray diffraction patterns of the FSM-16s treated with SCF-CO₂ (a) before, and (b) after, calcination at 773 K. Indexes corresponding to anatase crystal are noted.

ETS-10²⁰ could not be observed. These results suggest that the titanium atoms were not taken into the silica framework, but that the titanium oxide grew on the surface of the mesoporous silica.

Conclusion

TTIP molecules solvated with liquid IPA and supercritical CO₂ easily penetrated into mesopores of diameter larger than 3.5 nm and reacted with the silanol group on the surface of the mesoporous silica to form TiO₂ layers by the following calcinations. On the other

(20) Anderson, M. W.; Terasaki, O.; Ohsuna, T.; Philippou, A.; MacKay, S. P.; Ferreira, A.; Rocha, J.; Lidin, S. *Nature* **1994**, *367*, 27.

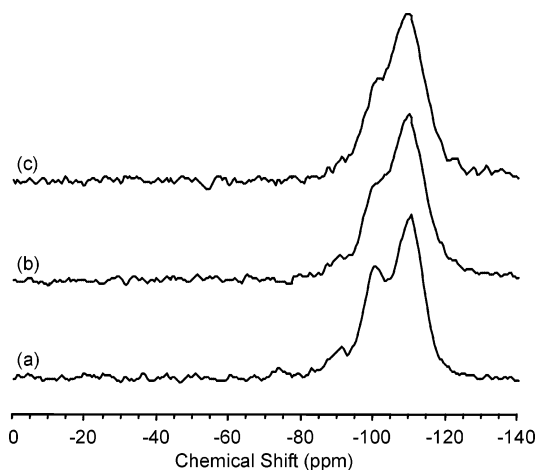


Figure 11. ²⁹Si MAS NMR spectra of the FSM-16s: (a) untreated sample; (b) sample treated with SCF-CO₂ solvent; (c) sample calcined after SCF-CO₂ treatment. A chemical shift δ was the measured with respect to a tetramethylsilane.

hand, the treated TTIP molecules could not diffuse into pores of diameter less than 1.6 nm. When the mesoporous silica of pore size 2.3 or 2.7 nm was used, penetration of TTIP with the supercritical CO₂ was permitted with some restriction, but that with the liquid IPA was still forbidden. These results were explained not only by the relation between the pore diameter and the size of the TTIP solvated with the solvent molecules, but also by the interaction of the solvent molecules with the silanol groups on the silica wall surfaces.

Acknowledgment. We gratefully acknowledge Dr. Norihiko Setoyama for the discussions to interpret the adsorption of N₂ for mesoporous silicas.

CM034422U